Journal of Applied Mechanics Vol.7,pp.15-20 (August 2004) JSCE

Stress concentration factor and scattering cross-section for plane SH-wave scattering by a circular cavity in a pre-stressed elastic medium

Sasikorn Leungvichcharoen* and Anil C. Wijeyewickrema**

* Doctoral Student, Dept. of Civil Eng., Tokyo Institute of Technology, O-okayama, Meguro-ku, Tokyo 152-8552
** Assoc. Professor, Dept. of Civil Eng., Tokyo Institute of Technology, O-okayama, Meguro-ku, Tokyo 152-8552

The effect of pre-stress on the scattering of plane SH-waves from a circular cylindrical cavity in a compressible isotropic elastic medium, is studied. The complex function method is employed to analyze the incremental boundary value problem. The spatial variables (x_1, x_2) are mapped onto two different complex planes so that the series solution of the incident waves and the scattered waves are expressed as functions of two different complex variables. The coefficient of each term in the series solution can be computed numerically from a set of linear simultaneous equations, which are constructed by satisfying the incremental traction-free boundary condition along the surface of the cavity. Varga material is assumed in the numerical examples. Varying the principal stretches, the effect of pre-stress on the dynamic stress concentration factor and the scattered energy is investigated.

Key Words: *complex function method, pre-stressed elastic media, circular cavity, SH-waves, scattering*

1. Introduction

Analysis of wave scattering in elastic media is very useful in engineering practice, for example calculation of soil-structure interaction due to seismic waves and non-destructive evaluation of structural components. A comprehensive study of wave scattering from a cavity or elastic body in a linear isotropic elastic medium can be found in the monograph by Pao and Mow[1]. Scattering problems in linear anisotropic elastic media have been considered by many authors[2)-6)].

If in certain situations the elastic medium can be initially pre-stressed by external static forces before the propagation of incident waves, then the dynamic analysis in a pre-stressed medium will be more appropriate, than the classical linear analysis. In the last two decades, wave propagation problems in pre-stressed elastic media have been extensively studied but due to the complexity of the analysis, which comes from the effects of pre-stress, analytical results of wave reflection and scattering problems, have been limited to reflection of waves from a linear plane boundary or interface only.[7),8)]

Recently, SH-wave scattering from a circular cylindrical cavity in a compressible pre-stressed unbounded elastic medium has been studied by the authors[9]. It was the first time that an elastic scattering problem in a pre-stressed medium has been considered. Since, the governing equation for anti-plane deformation of pre-stress media are mathematically identical with the governing equation of linear orthotropic elastic media, the complex function method used in the solution of dynamic stress concentration around a cavity in an infinite linear anisotropic elastic medium[2),3)] can be applied to the present pre-stress problem. Using the complex function method, the effect of pre-stress on the speed of incident body waves and the dynamic stress concentration factor (SCF) along the surface of the cavity has been explored. In the present paper, a further study of[9)] is carried out where more details of the SCF, the intensity of scattered energy and the scattering cross-section are included. The fundamental equations and formulation of the problem are given in Secs. 2 and 3. Numerical results of two examples when the Varga strain energy function is assumed have been given in Sec. 4.

¶ Dedicated to the memory of Prof. Michihiro KITAHARA

2. Basic Equations

Consider a homogeneous compressible isotropic elastic material with an initial unstressed state denoted by $\mathcal{B}_u$, which after being subjected to pure homogeneous strains has the new configuration $\mathcal{B}_e$, the pre-stressed equilibrium state. A Cartesian co-ordinate system $Ox_1x_2x_3$, with axes coincident with the principal axes of strain, is chosen for the configuration $\mathcal{B}_e$. Let $\mathbf{u}$ be a small, time dependent displacement superimposed on $\mathcal{B}_e$. The incremental equations of motion for small time dependent displacements superimposed on the finite quasi-static deformation and the component of incremental nominal stress tensor $\mathbf{s}_0$, can be written as (see Ch. 6 of[10)])

$$\mathcal{A}_{0jikl}u_{l,jk} = \rho\ddot{u}_i, \qquad s_{0ji} = \mathcal{A}_{0jilk}u_{k,l}, \tag{1}$$

where $\mathcal{A}_{0jilk}$ are the components of the fourth-order tensor of first-order instantaneous elastic moduli which relates the nominal stress increment tensor and the deformation gradient increment tensor, ρ is the material density in the current configuration and superimposed dot and comma indicate differentiation with respect to time t and spatial coordinate component in B_e, respectively.
The corresponding equations for anti-plane deformation where $u_3 = u_3(x_1, x_2, t)$ and $u_1 = u_2 = 0$ can be written as

$$\begin{aligned} &\mathcal{A}_{01313}u_{3,11} + \mathcal{A}_{02323}u_{3,22} = \rho\ddot{u}_3, \\ &s_{013} = \mathcal{A}_{01313}u_{3,1}, \quad s_{023} = \mathcal{A}_{02323}u_{3,2}, \end{aligned} \tag{2}$$

since $\mathcal{A}_{0i3j3}=0$ when $i \neq j$ (see Eq. 3.6 of [11]). The instantaneous elastic moduli $\mathcal{A}_{01313}$ and $\mathcal{A}_{02323}$ are given in term of the strain energy function $W(\lambda_1,\lambda_2,\lambda_3)$ and the principal stretches $\lambda_1,\lambda_2,\lambda_3$ as,

$$J\mathcal{A}_{0i3i3}=\begin{cases}(\lambda_i W_i-\lambda_3 W_3)\lambda_i^2/(\lambda_i^2-\lambda_3^2), & \lambda_i \neq \lambda_3 \\ \frac{1}{2}(\lambda_i^2 W_{ii}-\lambda_i\lambda_3 W_{i3}+\lambda_i W_i), & \lambda_i=\lambda_3,\end{cases} \quad (i=1,2) \tag{3}$$

where $W_i=\partial W/\partial\lambda_i, W_{ij}=\partial^2 W/\partial\lambda_i\partial\lambda_j, (i=1,2 \text{ and } j=1,3)$ and $J=\lambda_1\lambda_2\lambda_3$ [11].

The incremental nominal stress components s_{0rz} and $s_{0\theta z}$ in the cylindrical coordinate system (r,θ,z) where $x_1=r\cos\theta$, $x_2=r\sin\theta$ and $x_3=z$ can be expressed as,

$$\begin{aligned}s_{0rz}&=\mathcal{A}_{01313}u_{z,1}\cos\theta+\mathcal{A}_{02323}u_{z,2}\sin\theta,\\ s_{0\theta z}&=-\mathcal{A}_{01313}u_{z,1}\sin\theta+\mathcal{A}_{02323}u_{z,2}\cos\theta.\end{aligned} \tag{4}$$

Since the complex function method is used, the complex expression of non-dimensional stresses are obtained from Eq. (4) as,

$$\begin{aligned}\hat{s}_{0rz}-i\hat{s}_{0\theta z}&=[\gamma^2 u_{z,1}-iu_{z,2}]\mathrm{e}^{i\theta},\\ \hat{s}_{0rz}+i\hat{s}_{0\theta z}&=[\gamma^2 u_{z,1}+iu_{z,2}]\mathrm{e}^{-i\theta},\end{aligned} \tag{5}$$

where $\gamma^2=\mathcal{A}_{01313}/\mathcal{A}_{02323}$, $\hat{s}_{0rz}=s_{0rz}/\mathcal{A}_{02323}$ and $\hat{s}_{0\theta z}=s_{0\theta z}/\mathcal{A}_{02323}$.

3. Scattering of SH-Waves by a Circular Cylindrical Cavity

Consider an infinitely long circular cylindrical cavity in an unbounded pre-stressed elastic solid as shown in Fig. 1. The homogeneous principal stretches $\lambda_i, (i=1,2,3)$ yield the corresponding homogeneous static principal Cauchy stresses $\sigma_i, (i=1,2,3)$ (pg. 216 of [10]) and are given by,

$$\sigma_i=\lambda_i W_i/J, \quad (i=1,2,3). \tag{6}$$

Since the assumed homogeneous principal stretches yield homogeneous Cauchy stresses, the internal static traction that should be applied along the inner surface of the cavity is

$$\mathbf{t}_0(\theta)=-(\sigma_1\cos^2\theta+\sigma_2\sin^2\theta)\mathbf{e}_r+(\sigma_1-\sigma_2)\cos\theta\sin\theta\,\mathbf{e}_\theta, \tag{7}$$

where $\mathbf{e}_r$ and $\mathbf{e}_\theta$ are unit basis vectors. For the *equibiaxially* pre-stressed case $\sigma_1=\sigma_2$, the traction $\mathbf{t}_0(\theta)$ in Eq. (7) corresponds to an internal static pressure (i.e., $p_0=-\sigma_1$). In practice it is more natural to expect that if there are no tractions applied along the inner surface that there will be stress concentration in the pre-stressed state around the cavity.

3.1 Incident Wave

The incremental displacement of the incident time harmonic plane SH-wave $u_z^{(i)}(x_1,x_2,t)=U_0\mathrm{e}^{-i\omega t}\mathrm{e}^{ik_\alpha(x_1\cos\alpha+x_2\sin\alpha)}$ can be expressed in the polar coordinate system as

$$u_z^{(i)}(r,\theta,t)=U_0\mathrm{e}^{-i\omega t}\mathrm{e}^{ik_\alpha r\cos(\theta-\alpha)}, \tag{8}$$

where $\theta=\alpha$ is the direction of wave propagation, ω is angular frequency, $k_\alpha=\omega/c_\alpha$ is wavenumber, and c_α is wave speed in this direction, i.e., $\rho c_\alpha^2=\mathcal{A}_{01313}\cos^2\alpha+\mathcal{A}_{02323}\sin^2\alpha$ (pg. 474 of [10]). Here the superscript (i) indicates the incident wave.

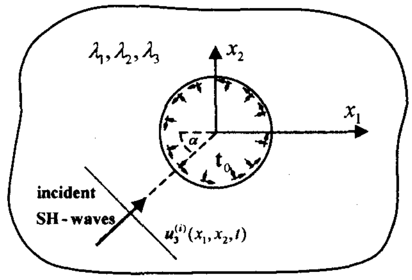

Fig. 1. Unbounded pre-stressed material with circular cylindrical cavity and the incident plane SH-wave.

Equation (8) may be expressed in the form of a Fourier series expansion[2] as,

$$u_z^{(i)}(r,\theta,t)=U_0\mathrm{e}^{-i\omega t}\sum_{n=-\infty}^{\infty} i^n\mathrm{e}^{in(\theta-\alpha)}J_n(k_\alpha r) \tag{9}$$

where J_n is the Bessel function of order n.

To use the complex function method introduce the complex variables,

$$\varsigma=x_1+ix_2=r\mathrm{e}^{i\theta},\ \bar{\varsigma}=x_1-ix_2=r\mathrm{e}^{-i\theta},\ |\varsigma|=r, \tag{10}$$

which yields,

$$u_{z,1}^{(i)}=u_{z,\varsigma}^{(i)}+u_{z,\bar{\varsigma}}^{(i)},\quad u_{z,2}^{(i)}=i(u_{z,\varsigma}^{(i)}-u_{z,\bar{\varsigma}}^{(i)}), \tag{11}$$

where $u_{z,\varsigma}^{(i)}=\partial u_z^{(i)}/\partial\varsigma$ and $u_{z,\bar{\varsigma}}^{(i)}=\partial u_z^{(i)}/\partial\bar{\varsigma}$, from which Eq. (9) can be expressed as

$$u_z^{(i)}(\varsigma,t)=U_0\mathrm{e}^{-i\omega t}\sum_{n=-\infty}^{\infty} i^n\mathrm{e}^{-in\alpha}J_n(k_\alpha|\varsigma|)(\varsigma/|\varsigma|)^n. \tag{12}$$

From Eqs. (5), (11) and (12) the stress components due to the incident wave can be written as

$$\begin{aligned}\hat{s}_{0rz}^{(i)}(\varsigma,t)=\frac{U_0k_\alpha\mathrm{e}^{-i\omega t}}{4}\Big\{&[(\gamma^2+1)\mathrm{e}^{i\theta}+(\gamma^2-1)\mathrm{e}^{-i\theta}]\\ &\sum_{n=-\infty}^{\infty} i^n\mathrm{e}^{-in\alpha}J_{n-1}(k_\alpha|\varsigma|)(\tfrac{\varsigma}{|\varsigma|})^{n-1}-[(\gamma^2-1)\mathrm{e}^{i\theta}+(\gamma^2+1)\mathrm{e}^{-i\theta}]\\ &\sum_{n=-\infty}^{\infty} i^n\mathrm{e}^{-in\alpha}J_{n+1}(k_\alpha|\varsigma|)(\tfrac{\varsigma}{|\varsigma|})^{n+1}\Big\},\\ \hat{s}_{0\theta z}^{(i)}(z,t)=\frac{iU_0k_\alpha\mathrm{e}^{-i\omega t}}{4}\Big\{&[(\gamma^2+1)\mathrm{e}^{i\theta}-(\gamma^2-1)\mathrm{e}^{-i\theta}]\\ &\sum_{n=-\infty}^{\infty} i^n\mathrm{e}^{-in\alpha}J_{n-1}(k_\alpha|\varsigma|)(\tfrac{\varsigma}{|\varsigma|})^{n-1}-[(\gamma^2-1)\mathrm{e}^{i\theta}-(\gamma^2+1)\mathrm{e}^{-i\theta}]\\ &\sum_{n=-\infty}^{\infty} i^n\mathrm{e}^{-in\alpha}J_{n+1}(k_\alpha|\varsigma|)(\tfrac{\varsigma}{|\varsigma|})^{n+1}\Big\}.\end{aligned} \tag{13}$$

3.2 Scattered Wave

When the incident wave $u_z^{(i)}$ impinges on the surface of the cavity, the scattered wave $u_z^{(s)}$ is generated and the total displacement is the summation of both incident and scattered waves i.e., $u_z = u_z^{(i)} + u_z^{(s)}$. For the scattered wave, another set of complex variables is introduced, i.e.,

$$\eta = x_1 + i\gamma x_2 = r(\cos\theta + i\gamma\sin\theta),\quad \bar{\eta} = x_1 - i\gamma x_2 = r(\cos\theta - i\gamma\sin\theta), \tag{14}$$

and hence,

$$u_{z,1}^{(s)} = u_{z,\eta}^{(s)} + u_{z,\bar{\eta}}^{(s)},\quad u_{z,2}^{(s)} = i\gamma(u_{z,\eta}^{(s)} - u_{z,\bar{\eta}}^{(s)}),$$
$$u_{z,11}^{(s)} = u_{z,\eta\eta}^{(s)} + 2u_{z,\eta\bar{\eta}}^{(s)} + u_{z,\bar{\eta}\bar{\eta}}^{(s)}, \tag{15}$$
$$u_{z,22}^{(s)} = -\gamma^2(u_{z,\eta\eta}^{(s)} - 2u_{z,\eta\bar{\eta}}^{(s)} + u_{z,\bar{\eta}\bar{\eta}}^{(s)}).$$

Substituting Eq. (15) into Eq. (2a) yields

$$4c_0^2 u_{z,\eta\bar{\eta}}^{(s)} = \ddot{u}_z^{(s)}, \tag{16}$$

where c_0 is the SH-wave speed in x_1-direction i.e., $\rho c_0^2 = \mathcal{A}_{01313}$.

Following the work of Liu et al.[12] the solution of Eq. (16), which satisfies the radiation condition when $r \to \infty$ can be written as

$$u_z^{(s)}(\eta,t) = \mathrm{e}^{-i\omega t}\sum_{n=-\infty}^{\infty} A_n H_n^{(1)}(k_0|\eta|)(\eta/|\eta|)^n, \tag{17}$$

where A_n, $n = 0, \pm1, \pm2, \ldots$ are arbitrary constants and $H_n^{(1)}$ is the Hankel function of order n and $k_0 = \omega / c_0$.

The corresponding stress components are

$$\hat{s}_{0rz}^{(s)}(\eta,t) = \tfrac{\gamma}{4}k_0\,\mathrm{e}^{-i\omega t}\sum_{n=-\infty}^{\infty}\{A_n[(\gamma+1)\mathrm{e}^{i\theta} + (\gamma-1)\mathrm{e}^{-i\theta}]\,H_{n-1}^{(1)}(k_0|\eta|)(\tfrac{\eta}{|\eta|})^{n-1} - [(\gamma-1)\mathrm{e}^{i\theta} + (\gamma+1)\mathrm{e}^{-i\theta}]\,H_{n+1}^{(1)}(k_0|\eta|)(\tfrac{\eta}{|\eta|})^{n+1}\},$$
$$\hat{s}_{0\theta z}^{(s)}(\eta,t) = \tfrac{i\gamma}{4}k_0\,\mathrm{e}^{-i\omega t}\sum_{n=-\infty}^{\infty}\{A_n[(\gamma+1)\mathrm{e}^{i\theta} - (\gamma-1)\mathrm{e}^{-i\theta}]\,H_{n-1}^{(1)}(k_0|\eta|)(\tfrac{\eta}{|\eta|})^{n-1} - [(\gamma-1)\mathrm{e}^{i\theta} - (\gamma+1)\mathrm{e}^{-i\theta}]\,H_{n+1}^{(1)}(k_0|\eta|)(\tfrac{\eta}{|\eta|})^{n+1}\}. \tag{18}$$

The incremental boundary condition along the surface of a circular cavity with radius *a* is expressed as

$$\hat{s}_{0rz}^{(i)}(\varsigma,t) + \hat{s}_{0rz}^{(s)}(\eta,t) = 0,\ \text{ on } |\varsigma| = a. \tag{19}$$

Substituting Eqs. (13) and (18) into Eq. (19) yields

$$\sum_{n=-\infty}^{\infty} A_n\phi_n = \phi, \tag{20}$$

where,

$$\phi_n = \tfrac{k_0\gamma}{k_\alpha}\{[(\gamma+1)\mathrm{e}^{i\theta} + (\gamma-1)\mathrm{e}^{-i\theta}]H_{n-1}^{(1)}(k_0|\eta|)(\tfrac{\eta}{|\eta|})^{n-1} - [(\gamma-1)\mathrm{e}^{i\theta} + (\gamma+1)\mathrm{e}^{-i\theta}]H_{n+1}^{(1)}(k_0|\eta|)(\tfrac{\eta}{|\eta|})^{n+1}\},$$
$$\phi = -[(\gamma^2+1)\mathrm{e}^{i\theta} + (\gamma^2-1)\mathrm{e}^{-i\theta}]\sum_{n=-\infty}^{\infty}(i)^n\,\mathrm{e}^{-in\alpha}J_{n-1}(k_\alpha|\varsigma|)(\tfrac{\varsigma}{|\varsigma|})^{n-1} + [(\gamma^2-1)\mathrm{e}^{i\theta} + (\gamma^2+1)\mathrm{e}^{-i\theta}]\sum_{n=-\infty}^{\infty}(i)^n\,\mathrm{e}^{-in\alpha}J_{n+1}(k_\alpha|\varsigma|)(\tfrac{\varsigma}{|\varsigma|})^{n+1},$$

on $|\varsigma| = a$. (21)

Multiplying both sides of Eq. (20) with $\mathrm{e}^{-im\theta}$ and integrating from $-\pi$ to π yields a set of simultaneous equations:

$$\sum_{n=-\infty}^{\infty} A_n\phi_{mn} = \phi_m,\quad m = 0, \pm1, \pm2, \ldots \tag{22}$$

where $\phi_{mn} = \frac{1}{2\pi}\int_{\theta=-\pi}^{\pi}\phi_n\mathrm{e}^{-im\theta}d\theta$ and $\phi_m = \frac{1}{2\pi}\int_{\theta=-\pi}^{\pi}\phi\,\mathrm{e}^{-im\theta}d\theta$.
The coefficients A_n, $n = 0, \pm1, \pm2, \ldots$ can be determined numerically by replacing the infinite series in Eq. (22) by a finite series and solving the corresponding system of simultaneous equations. A convergent solution can be obtained by increasing the number of terms considered in the finite series.

3.3 Dynamic Stress Concentration Factor

Along the surface of the cavity, the dynamic stress concentration factor is defined as the ratio of incremental stress amplitude $|s_{0\theta z}|$ to the maximum amplitude of the incident incremental stress at the same point. For time harmonic incident SH-wave given in Eq. (8), the maximum amplitude of the incident shear stress is

$$\max(s_{\theta z}^{(i)}) = \mathcal{A}_{02323}k_\alpha U_0\left|-\gamma^2\cos\alpha\sin\theta' + \sin\alpha\cos\theta'\right| \tag{23}$$

where $\theta' = \arctan(-\gamma^2\cot\alpha)$. Therefore the dynamic stress concentration factor can be expressed as

$$\mathrm{SCF} = \left|\frac{\hat{s}_{0\theta z}^{(i)} + \hat{s}_{0\theta z}^{(s)}}{k_\alpha U_0(\sin\alpha\cos\theta' - \gamma^2\cos\alpha\sin\theta')}\right|. \tag{24}$$

In the absence of pre-stress $\mathcal{A}_{01313} = \mathcal{A}_{02323} = \mu_0$ and $\gamma^2 = 1$, and Eq. (23) is reduced to $\max(s_{\theta' z}^{(i)}) = \mu_0 k_\alpha U_0$ which agrees with linear isotropic case (page 132 of[1]).

3.4 Scattered Energy

The time average of energy flow can be calculated from either the real or imaginary part of stress and displacement e.g.,

$$\mathrm{Ave}(\dot{\mathrm{E}}) = \tfrac{1}{T}\int_0^T\iint_A \mathrm{Re}[s_{i3}]\mathrm{Re}[\dot{u}_z]n_i dA\,dt = \tfrac{1}{4T}\int_0^T\iint_A (s_{i3} + \bar{s}_{i3})(\dot{u}_z + \bar{\dot{u}}_z)n_i dA\,dt, \tag{25}$$

where $\bar{s}_{i3}$ and $\bar{\dot{u}}_z$ are complex conjugates of s_{i3} and $\dot{u}_z$, respectively. For time harmonic waves (see Eqs. (8) and (17)), which has period $T = 2\pi/\omega$ since $\int_0^T \mathrm{e}^{-2i\omega t}dt = 0$ the above equation reduced to

$$\mathrm{Ave}(\dot{\mathrm{E}}) = -\tfrac{i\omega}{4}\mathcal{A}_{02323}\iint_A (S_{i3}\bar{U}_z - \bar{S}_{i3}U_z)n_i dA, \tag{26}$$

where $s_{i3} = \mathcal{A}_{02323}S_{i3}\mathrm{e}^{-i\omega t}$, $u_z = U_z\mathrm{e}^{-i\omega t}$ and $\bar{S}_{i3}$ and $\bar{U}_z$ are complex conjugate of S_{i3} and U_z respectively.

The average of energy flux per unit area normal to the propagation direction of plane incident waves shown in Eq. (8) is

$$\mathrm{Ave}(\dot{e}^{(i)}) = \mathrm{Ave}(\dot{E}^{(i)})/A, \quad = \tfrac{1}{2}k_\alpha \omega \mathcal{A}_{02323} U_0^2(\gamma^2\cos^2\alpha + \sin^2\alpha). \tag{27}$$

For a circular cavity, the total scattered energy per unit length of cylindrical surface at radius r is

$$\mathrm{Ave}(\dot{E}^{(s)}) = -\tfrac{1}{4}i\omega\mathcal{A}_{02323}\int_{\theta=0}^{2\pi}[S_{rz}^{(s)}\bar{U}_z^{(s)} - \bar{S}_{rz}^{(s)}U_z^{(s)}]rd\theta, \tag{28}$$

where the average energy flux across a cylindrical surface is,

$$\mathrm{Ave}(\dot{e}^{(s)}) = -\tfrac{1}{4}i\omega\mathcal{A}_{02323}[S_{rz}^{(s)}\bar{U}_z^{(s)} - \bar{S}_{rz}^{(s)}U_z^{(s)}]. \tag{29}$$

The ratio $\mathrm{Ave}(\dot{E}^{(s)})/\mathrm{Ave}(\dot{e}^{(i)})$ has the dimension of area per unit length of cylinder and is referred as *scattering cross-section* when $k_\alpha r \to \infty$ (page 138 of [1]) i.e.,

$$\Sigma = \lim_{k_\alpha r\to\infty}[\mathrm{Ave}(\dot{E}^{(s)})]/\mathrm{Ave}(\dot{e}^{(i)}), \tag{30}$$

where $-\tfrac{1}{4}i\omega r\mathcal{A}_{02323}[S_{rz}^{(s)}\bar{U}_z^{(s)} - \bar{S}_{rz}^{(s)}U_z^{(s)}]$ is the scattered energy flux per unit area (page 138 of [1]) and its intensity ratio Λ is given by

$$\Lambda = \lim_{k_\alpha r\to\infty}[r\,\mathrm{Ave}(\dot{e}^{(s)})]/\mathrm{Ave}(\dot{e}^{(i)}). \tag{31}$$

4. Numerical Results

As mentioned in Sec. 2 the instantaneous elastic moduli $\mathcal{A}_{01313}$ and $\mathcal{A}_{02323}$ depend on the strain energy function of the material and the principal stretches. In this section compressible Varga material is assumed and the strain energy function is given by [11],

$$W^{(V)} = 2\mu_0[\lambda_1 + \lambda_2 + \lambda_3 - 3 - \ln(\lambda_1\lambda_2\lambda_3)]. \tag{32}$$

From the definition of $\mathcal{A}_{01313}$, $\mathcal{A}_{02323}$, and γ (see Sec. 2), Eq. (32) yields

$$J\mathcal{A}_{01313} = 2\mu_0\lambda_1^2/(\lambda_1+\lambda_3), \quad J\mathcal{A}_{02323} = 2\mu_0\lambda_2^2/(\lambda_2+\lambda_3), \quad \gamma = \frac{\lambda_1}{\lambda_2}\sqrt{\frac{\lambda_2+\lambda_3}{\lambda_1+\lambda_3}}. \tag{33}$$

For the pre-stressed material which is *equibiaxially* deformed in (x_1x_2)-plane (i.e., $\lambda_1 = \lambda_2 = \lambda$), Eq. (33) yields $\mathcal{A}_{01313} = \mathcal{A}_{02323} = \mu$ and $\gamma = 1$, where $\mu = 2\mu_0\lambda^2/J(\lambda+\lambda_3)$ is the shear stiffness of the material in the equilibrium configuration. From the orthogonal properties of $e^{-im\theta}$, $m = 0, \pm 1, \pm 2, \ldots$ the linear-isotropic-like solution (pg. 121 of [1]) is recovered and the coefficient A_n in Eq. (22) can be expressed as

$$A_n = -i^n\frac{nJ_n(ka) - kaJ_{n+1}(ka)}{nH_n^{(1)}(ka) - ka\,H_n^{(1)}(ka)}, \quad (n = 0, \pm 1, \pm 2, \ldots), \tag{34}$$

where

$$ka = \omega a\sqrt{\rho/\mu}, \quad \rho = \rho_0/J, \quad a = a_0\lambda^2, \tag{35}$$

are non-dimensional wavenumber, material density and radius of cavity in equilibrium configuration, respectively. In Eq. (35) ρ_0 is material density and a_0 is radius of cavity in the natural un-stressed configuration. Since $\gamma = 1$, it can be seen from Eqs. (13), (18), (24) and (34) that the dynamic stress concentration factor does not explicitly depend on stretches $\lambda_1 = \lambda_2$ and λ_3 i.e., for the same value of ka. In addition, the scattered energy intensity and scattering cross-section depend implicitly on ka.

The prescribed parameters of Examples 1 and 2 are the same with [9], but here the additional results e.g., scattered energy intensity and scattering cross-section have been included and discussed in detail.

Example 1:

Figure 2 shows the geometry of this example when the compressible Varga material is *equibiaxially* deformed in (x_1x_2)-plane (i.e., $\lambda_1 = \lambda_2 = \lambda$) and the internal pressure $p_0 = 2\mu_0(1-\lambda)/J$ is applied inside the cavity. The internal pressure is necessary since homogeneous stretches are assumed. The incident wave is assumed to propagate in the x_1-direction. The non-dimensional phase speed of the SH- wave $\bar{c} = \sqrt{\mu\rho_0/\mu_0\rho}$ which depends on the values of principal stretches is shown in Fig. 3.

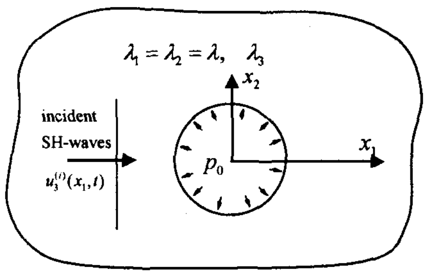

Fig. 2. Geometry of Example 1.

It can be seen in Fig. 3 that for $\lambda_3 < \lambda < 1.0$ which simulates the pre-stressed earth when the (x_1x_2)-plane is parallel to the horizontal ground surface, the speed of SH-waves is slower than that of the non pre-stressed material i.e., $\bar{c} < 1.0$.

The plot of dynamic stress concentration factors when $ka = 0.1, 1$ and 2 is shown in Fig. 4. Since the (x_1x_3)-plane is a plane of symmetry, SCF is plotted for $0° \le \theta \le 180°$. It is seen from Figs. 4 and 5 that the dynamic stress concentration factor and max(SCF) obtained in this example is equivalent to the linear isotropic case (pg. 134 of [1]) when ka is replaced by $k_0a_0 = \omega a_0\sqrt{\rho_0/\mu_0}$.

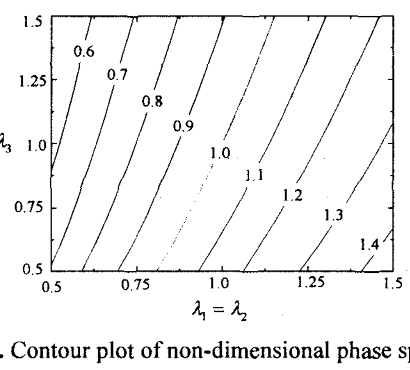

Fig. 3. Contour plot of non-dimensional phase speed

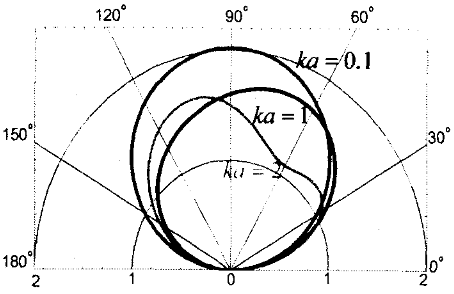

Fig. 4. Dynamic stress concentration factor SCF of Example 1.

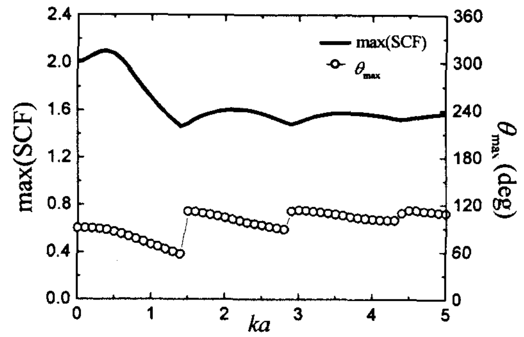

Fig. 5. Maximum value of stress concentration factor SCF and the angle of its position θ_{max}.

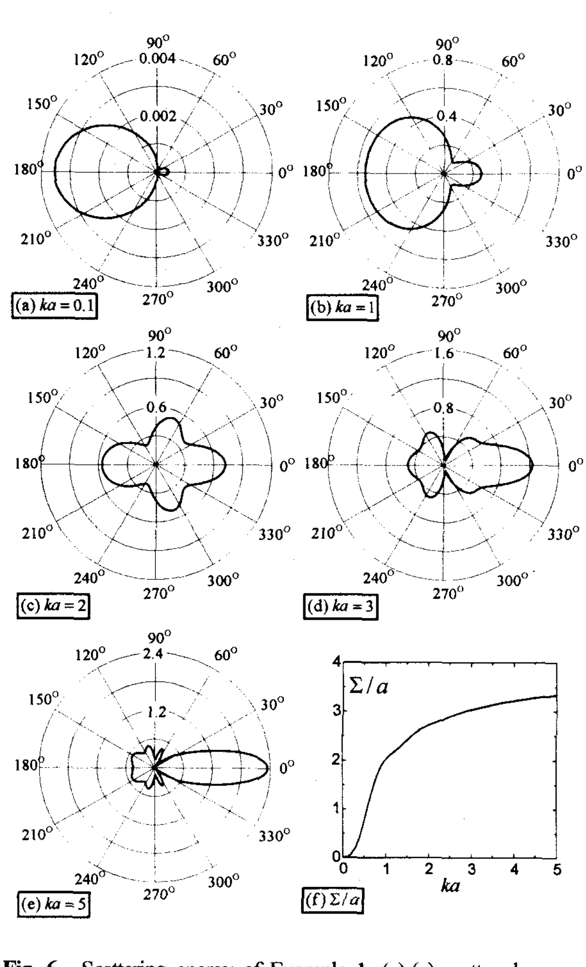

Fig. 6. Scattering energy of Example 1; (a)-(e) scattered energy intensity ratio Λ / a ; (f) non-dimensional scattering cross-section Σ / a.

Figure 5 shows the maximum values of stress concentration factor $\max(\text{SCF})$ and its location θ_{max}. It can be seen that when ka gradually increases from 0, $\max(\text{SCF})$ increase from 2.0 until it reaches the peak at $ka = 0.4$ when $\max(\text{SCF}) = 2.1$. This was also discussed in [1] for the linear isotropic case. For small ka, $\theta_{max} \le 90^{\circ}$ while $\theta_{max} > 90^{\circ}$ when ka is high enough.

In Fig. 6 the scattered energy intensity ratio Λ and the scattering cross-section Σ are plotted. It can be seen when ka is small, Λ is almost uniformly distributed in all the backward directions and, when ka is high Λ is mostly in the forward direction with a concentrated peak at $\theta = 0^{\circ}$. The behavior of Σ is clearly shown in Fig. 6(f).

Example 2:

The compressible Varga material is *equibiaxially* deformed in the $(x_1 x_3)$ -plane with principal stretches $\lambda_1 = \lambda_3 = \lambda = 0.9$ and $\lambda_2 = 0.8$, where the internal static traction $\mathbf{t}_0(\theta) = 3.527\mu_0 \quad [(3\cos^2\theta + \sin^2\theta)\mathbf{e}_r - \sin 2\theta\, \mathbf{e}_\theta]$ is applied along the inner surface of the cavity since uniform stretches are assumed. It is noted here that λ_2 was erroneously given as $\lambda_2 = 0.7$ in [9]. The incident SH-wave has an incident angle $\alpha = 45^{\circ}$ (see Fig. 1). Using the method presented in Sec. 2 and truncating the series in Eq. (22) at $n = \pm n_{max}$ yields a set of simultaneous $2n_{max} + 1$ equations. The coefficient A_n, $n = 0, \pm 1, \pm 2, \ldots, \pm n_{max}$ can be obtained by solving the resulting system of equations. In this example it is found that a convergent solution is obtained when the series is truncated at $n_{max} = 8$.

The scattering cross-section, $\max(\text{SCF})$ and its location are plotted for $0 < k_\alpha a < 5.0$ in Fig. 7. The behavior of Σ and $\max(\text{SCF})$ are similar to Example 1 while θ_{max} is different since the problem is not symmetric like Example 1.

The real and imaginary parts of the amplitude of the displacement and shear stresses along the surface of the cavity, the distribution of SCF and scattered energy intensity Λ are plotted in Fig. 8.

Figures 8(a) and (c) can be used to calculate the displacement and shear stresses at any time in the period of vibration, while Fig. 8 (b) shows that the results agree with the boundary condition at the surface of the cavity. It is seen from Fig. 8(d) and (e) that the distribution of SCF and Λ are not symmetric with respect to any plane or axis, this effect cannot be seen for the in-plane equibiaxial pre-stress case (Example 1) and for linear isotropic case.

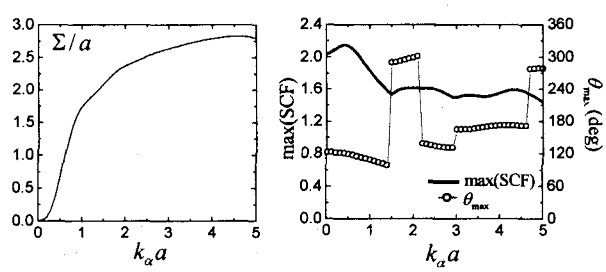

Fig. 7. Non-dimensional scattering cross-section and the maximum value of stress concentration factor of Example 2.

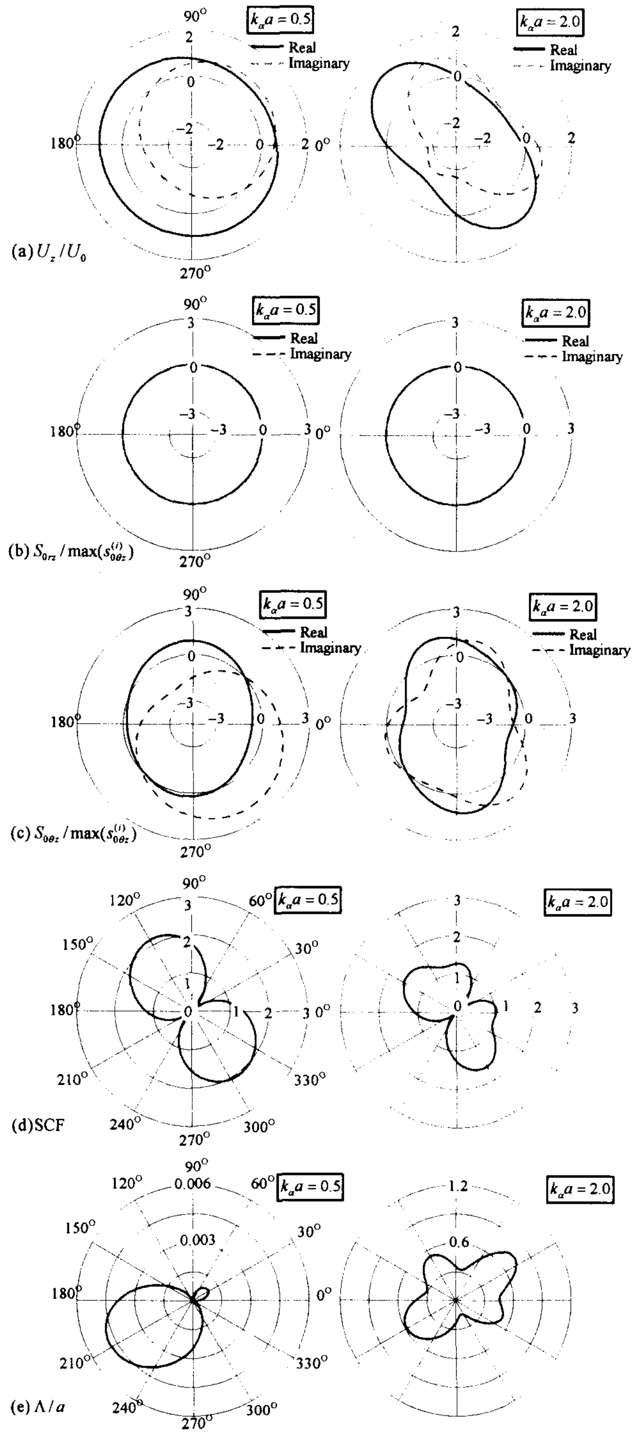

Fig. 8. Results of Example 2 when $k_\alpha a = 0.5$ and 2.0; (a) displacement, (b)-(c) stresses, (d) stress concentration factor SCF and (e) scattered energy intensity ratio Λ / a.

5. Conclusions

Using the complex function method the scattering of plane SH-waves from a circular cylindrical cavity in a pre-stressed elastic medium is analyzed. The effect of pre-stress on the speed of plane SH-waves, the dynamic stress concentration factor, scattered energy intensity and scattering cross-section can be clearly seen from the numerical results. Long SH-waves will have a higher stress concentration than short SH-waves. The scattered energy intensity is less and mostly uniform in the backward direction for long SH-waves while for short SH-waves the higher energy intensity is scattered and it has a concentrated peak in the forward direction. The distribution of stress concentration factor and scattered energy intensity for pre-stressed media is not always symmetric, except for the in-plane equibiaxially deformed case. Scattering problems for non-circular cavities and inclusions in pre-stressed elastic unbounded media or in a half-space and the scattering of in-plane waves (P and SV waves) should also be studied.

Acknowledgements: The first author gratefully acknowledges financial support from 21st Century COE program "Evolution of Urban Earthquake Engineering", Tokyo Institute of Technology, Tokyo, Japan.

References

1) Pao, Y.-H. and Mow, C.-C. (1973), *Diffraction of Elastic Waves and Dynamic Stress Concentrations*, Crane-Russak, New York.
2) Liu, D. (1988), Dynamic stress concentration around a circular hole due to SH-wave in anisotropic media, *Acta Mechanica Sinica*, 4, pp. 146-155.
3) Liu, D. and Han, F. (1993), The scattering of plane SH-waves by noncircular cavity in anisotropic media, *J. Appl. Mech.*, 60, pp. 769-772.
4) Clements D. L. (1994), Surface motion of anisotropic and in-homogeneous alluvial valleys under incident plane SH waves, *IUTAM Symposium on Anisotropy, Inhomogeneity and Nonlinearity in Solid Mechanics*, Nottingham, U.K., 30 Aug-3 Sept 1994, pp. 449-454.
5) Han, F., Yan, W. and Liu, D. (1995), The interaction of plane SH-waves and circular cavity surfaced with lining in anisotropic Media, *Appl. Math. Mech.*, 16, pp. 1149-1159.
6) Niklasson A. J., and Datta S. K. (1998), Scattering by an infinite transversely istropic cylinder in a transversely isotropic medium. *Wave Motion*, 27, pp. 169-185.
7) Ogden R. W. and Sotiropoulos, D. A. (1998), Reflection of plane waves from the boundary of a pre-stressed compressible elastic half-space, *IMA J. Appl. Math.*, 61, pp. 61-90.
8) Hussain, W. and Ogden R. W. (2001), The effect of pre-strain on the reflection and transmission of plane waves at an elastic interface, *Int. J. Eng. Sci.*, 39, pp. 929-950.
9) Leungvichcharoen, S. and Wijeyewickrema, A. C. (2004), Scattering of Plane SH-waves by a circular cavity in a pre-stressed elastic medium, *First International Conference on Urban Earthquake Engineering*, Tokyo, Japan, 8-9 March 2004, pp. 501-508.
10) Ogden, R. W. (1984), *Non-linear Elastic Deformation*, Dover Publications, New York.
11) Roxburgh, D. G. and Ogden, R. W. (1994), Stability and vibration of pre-stressed compressible elastic plates, *Int. J. Eng. Sci.*, 32, pp. 427-457.
12) Liu, D., Gai, B. and Tao, G. (1982), Application of the method of complex functions to dynamic stress concentrations, *Wave Motion*, 4, pp. 293-304.

(Received: April 16, 2004)